

Estimation for bivariate quantile varying coefficient model

Linglong Kong*, Haoxu Shu, Giseon Heo*
Department of Mathematical and Statistical Sciences,
University of Alberta
Edmonton, AB T6G 2G1 Canada
and
Qianchuan He
Public Health Sciences Division,
Fred Hutchinson Cancer Research Center,
Seattle, WA 98109 USA

November 10, 2015

Abstract

We propose a bivariate quantile regression method for the bivariate varying coefficient model through a directional approach. The varying coefficients are approximated by the B-spline basis and an L_2 -type penalty is imposed to achieve desired smoothness. We develop a multistage estimation procedure based the Propagation-Separation (PS) approach to borrow information from nearby directions. The PS method is capable of handling the computational complexity raised by simultaneously considering multiple directions to efficiently estimate varying coefficients while guaranteeing certain smoothness along directions. We reformulate the optimization problem and solve it by the Alternating Direction Method of Multipliers (ADMM), which is implemented using R while the core is written in C to speed it up. Simulation studies are conducted to confirm the finite sample performance of our proposed method. A real data on Diffusion Tensor Imaging (DTI) properties from a clinical study on neurodevelopment is analyzed.

Keywords: bivariate quantile regression, varying coefficient model, Propagation-Separation (PS), Alternating Direction Method of Multipliers (ADMM), convex optimization, Diffusion Tensor Imaging (DTI).

*The authors gratefully acknowledge Natural Sciences and Engineering Research Council of Canada (*NSERC*). Heo's primary affiliation is in School of Dentistry, University of Alberta and is cross appointed in the Department of Mathematical and Statistical Sciences. Heo also acknowledges *McIntyre Memorial Funding* in Orthodontics division, School of Dentistry.

1 Introduction

Consider a regression model $Y_i = f(X_i, \beta) + \epsilon_i$, for $i = 1, \dots, n$, where Y_i represents the response, X_i is a vector of covariates, β is the regression coefficient parameter, f is a known or unknown function of the covariates X_i and β , and ϵ_i is the error term. Assuming a known function f , in the ordinary least square (OLS) regression, the parameter β is estimated by minimizing the sum of squared residuals $\sum_{i=1}^n (y_i - f(\mathbf{x}_i, \beta))^2$. While in quantile regression (QR), the QR effect β_τ for $\tau \in (0, 1)$ is obtained by minimizing

$$\sum_{i=1}^n \rho_\tau(y_i - f(\mathbf{x}_i, \beta)), \quad (1)$$

where $\rho_\tau(u) = u(\tau - I(u < 0))$ is the quantile loss function (Koenker and Bassett, 1978). When $\tau = .5$, the quantile regression becomes the least absolute deviation (LAD) regression, an alternative to the OLS, which estimates the conditional median instead the conditional mean of the response. By assuming that the error follows the asymmetric Laplace distribution, the maximum likelihood approach or Bayesian method can be used to estimate β (Yu and Moyeed, 2001; Yuan and Yin, 2010; Yang *et al.*, 2015).

There are at least three advantages to consider conditional quantiles instead of the conditional mean in a regression setting. First, quantile regression, in particular median regression, provides an alternative and complement to mean regression while being resistant to outliers in responses; in addition, quantile regression is more efficient than mean regression when the error follows a distribution with heavy tails. Second, quantile regression is capable of dealing with heteroscedasticity, the situation in which variances depend on certain covariates. More importantly, quantile regression can give a more complete picture on how the responses are affected by covariates, particularly the tail behavior of the response conditional on covariates, for example in economic and actuaries. For more background on quantile regression, see the monograph by Koenker (2005).

Inspired by the success of the univariate quantile (for a single response), researchers began to extend univariate quantiles to multivariate quantiles (i.e., for multiple responses). For example, the definition of multivariate quantile proposed by Chaudhuri (1996) is a generalization of what was proposed by Koenker and Bassett (1978) in univariate cases. In general, there is an associated multivariate median for any concept of multivariate quantiles.

In other words, we first solve for the multivariate median and then extend it to multivariate quantiles. There are many methods to define a multivariate median, for more details see Small (1990). Some methods for multivariate medians can be extended to multivariate quantiles, and different authors gave distinct multivariate quantile extensions, such as the spatial L_1 median Koltchinskii (1996) and the Oja median computed by Ronkainen *et al.* (2003). However, not every multivariate extension of quantiles can be obtained from a multivariate median. Alternatively, multivariate quantiles can be generalized directly from univariate quantiles (via approaches based on norm minimization), such as the one derived by Abdous and Theodorescu (1992).

The methods for univariate quantile regression are, in general, not easily applicable to multivariate quantile regression because of many reasons, one of which is the difficulty of interpretation. Nevertheless, multivariate quantiles via a directional approach is one of the successful extensions (Breckling and Chambers, 1988; Wei, 2008; Hallin *et al.*, 2010; Kong and Mizera, 2012). This approach was proposed and applied to bivariate growth charts by Kong and Mizera (2012). The authors showed that the analysis in terms of directional quantiles and their envelopes offers a straightforward probabilistic interpretation and thus conveys a concrete quantitative meaning. They also demonstrated that the directional quantile regression can facilitate the construction of bivariate growth charts and provide richer information than univariate growth charts.

Borrowing the ideas and notations from Kong and Mizera (2012), we explain directional quantile regression as follows. Let $\mathbf{S}^{\text{d}-1} = \{\mathbf{s} \in \mathbb{R}^{\text{d}} : \|\mathbf{s}\| = 1\}$ and X be a random vector in \mathbb{R}^{d} with distribution \mathbb{P} . Given $\mathbf{s} \in \mathbf{S}^{\text{d}-1}$ and $0 < \tau < 1$, the τ -th directional quantile in the direction \mathbf{s} is defined as the τ -th quantile of the corresponding projection of the distribution of X , that is,

$$Q(\tau, \mathbf{s}) = Q(\tau, \mathbf{s}^T X) = \inf\{u : \mathbb{P}(\mathbf{s}^T X \leq u) \geq \tau\}. \quad (2)$$

For fixed $\tau \in (0, 1/2]$, the τ -th directional quantile envelope generated by $Q(\tau, \mathbf{s})$ is defined as the intersection of halfspaces,

$$D(\tau) = \bigcap_{\mathbf{s} \in \mathbf{S}^{\text{d}-1}} H(\mathbf{s}, Q(\tau, \mathbf{s})), \quad (3)$$

where $H(\mathbf{s}, q) = \{x : \mathbf{s}^T x \geq q\}$ is the supporting halfspace determined by $\mathbf{s} \in \mathcal{S}^{d-1}$ and $q \in \mathbb{R}$. This multivariate directional quantile concept can be easily extended to multivariate directional quantile regression (Kong, 2009; Kong and Mizera, 2012). In general, given a direction \mathbf{s} and a multivariate regression model $\mathbf{Y} \sim \mathbf{f}(\mathbf{X}, \boldsymbol{\beta})$, where $\mathbf{Y} = (Y_1, \dots, Y_d)^T$, we project \mathbf{Y} on the direction \mathbf{s} and denote it as $\mathbf{Y}^* = \mathbf{s}^T \mathbf{Y}$. Then using data $\{(\mathbf{y}_i^*, \mathbf{x}_i)\}, i = 1, \dots, n$, for $0 < \tau < 1$, we can obtain the τ -th quantile by minimizing $\sum \rho_\tau(\mathbf{y}_i^* - \mathbf{f}(\mathbf{x}_i, \boldsymbol{\beta}_\tau))$, where $(\mathbf{y}_i, \mathbf{x}_i)$ are observations from (\mathbf{Y}, \mathbf{X}) . Similarly, we can have directional quantiles at any other selected directions. Using these quantiles, we can generate the τ -th conditional directional quantile envelope of \mathbf{Y} for any given \mathbf{X} . The directional quantile envelopes are essentially Tukey's depth contours (Tukey, 1975; Kong and Zuo, 2010) and the directional quantile regression envelopes are herein the conditional Tukey's depth contours. The directional quantile regression inherits good properties from Tukey's depth and also provides straightforward probabilistic interpretation; for more details, see (Kong, 2009; Kong and Mizera, 2012).

Since the varying coefficient model was systematically introduced by Hastie and Tibshirani (1993), it rapidly becomes a powerful statistical tool for time series and longitudinal data (Wu *et al.*, 1998; Huang *et al.*, 2002; Fan *et al.*, 2003). Recently, it has been developed for functional data analysis; see (Ramsay and Silverman, 2005; Zhang and Chen, 2007; Zhu *et al.*, 2012). In quantile regression literatures, there are also many new developments, for example, Honda (2004); Kim (2007); Cai and Xu (2008); Wang *et al.* (2009); Tang *et al.* (2013), and Zhao *et al.* (2013), just to name a few. However, in the functional data analysis framework, there are only limited methodologies available, for example, Zhou *et al.* (2015) developed a novel method for quantile regression with varying coefficients for univariate functional responses based on the local polynomial kernel smoothing technique. In real world, however, multiple measurements may be taken along a series of spatial or temporal points. For example, in diffusion tensor imaging (DTI) studies multiple fiber measurements like fractional anisotropy (FA) and mean diffusivity (MD) are measured along major fiber tracts (Zhu *et al.*, 2010, 2011, 2012). To jointly model the multiple functional responses with the spatial positions will enhance the strength shared among the responses and positions, and thus will improve the efficiency of the quantile estimates and provide more

information to reveal some underlying truth that can not be obtained by individual modeling. Unfortunately, there is no existing method in the literature that can handle such a task in the quantile regression with varying coefficients for functional responses.

In this article, we propose a novel estimation procedure in bivariate quantile varying coefficient model for functional responses to investigate the association between the responses and the covariates of interests, such as gender and gestational age (Zhu *et al.*, 2011). Our estimation method is based on the directional quantile concept and has the following innovative features. First, by jointly modeling the bivariate functional responses our method provides a conditional bivariate quantile envelope tube along the spatial or temporal positions which is capable of uncovering the underlying information that can not be obtained by univariate quantile regression. Second, to achieve the desired smoothness along the spatial or temporal positions for the quantile envelope tubes, an L_2 -type roughness penalty is imposed to estimate the varying coefficients approximated by B-splines (Koenker, 2005). Third, to improve the efficiency of the quantile estimates, we develop a multistage estimation procedure based on the propagation-separation (PS) approach (Polzehl and Spokoiny, 2000, 2006) to gradually borrow information from nearby directions with increasing number of directions. The PS method is capable of handling the computational complexity raised by simultaneously considering multiple directions to efficiently estimate varying coefficients while guaranteeing certain smoothness along directions. To the best of our knowledges, this is the first method to construct the directional quantile regression envelopes by simultaneously considering multiple directions. Forth, we reformulate the optimization problem and solve it by the Alternating Direction Method of Multipliers (ADMM) repopularized by Boyd *et al.* (2011), which is implemented using R while the core is written in C to speed it up. ADMM is efficient to tackle our optimization problem with a nonsmooth quantile loss function plus a L_2 type penalty.

We organize our article as follows. We introduce the bivariate quantile varying coefficient model and define the objective function with penalties by approximating the varying coefficients using B-splines in Section 2.1. We adapt the PS approach to our estimation and describe the multistage estimation procedures for varying coefficients in Section 2.2. In Section 2.3, we reformulate the optimization problem and solve it by ADMM. Our proposed

estimation procedure and algorithm are examined in the simulation studies in Section 3.1. As a demonstration, fractional anisotropy (FA) and mean diffusivity (MD) along the genu fiber bundle of the corpus callosum (GCC) of the diffusion tensor imaging (DTI) from a clinical study on neurodevelopment are analyzed in Section 3.2. We summarize our results and discuss future work in Section 4.

2 Methodology

2.1 Bivariate quantile varying coefficient model

Motivated by the generalized regression quantiles of Guo *et al.* (2015) and the multivariate varying coefficient model in Zhu *et al.* (2011), we propose our bivariate quantile varying coefficient model (BQVCM) through a directional quantile approach (Kong, 2009; Kong and Mizera, 2012). Let $\mathbf{Y}(t) = (Y_1(t), Y_2(t))^T \in \mathbb{R}^2$ be a bivariate functional response at time t , where $t \in [0, 1]$, and $\mathbf{X} \in \mathbb{R}^p$ be the covariates of interest. For fixed $0 < \tau < 1$, given a direction $\mathbf{s} \in \mathcal{S}^1$, the bivariate quantile varying coefficient model defines the τ -th directional quantile of $\mathbf{Y}(t)$ at t given \mathbf{X} , denoted by $Q_{\mathbf{Y}(t)|\mathbf{X}}(\tau, \mathbf{s})$,

$$Q_{\mathbf{Y}(t)|\mathbf{X}}(\tau, \mathbf{s}) = \mathbf{f}(\mathbf{X}, \boldsymbol{\beta}_\tau(\mathbf{s}, t)), \quad (4)$$

where \mathbf{f} characterizes the dependency of the quantile of $\mathbf{Y}(t)$ on \mathbf{X} and the varying coefficients $\boldsymbol{\beta}_\tau(\mathbf{s}, t)$ are the τ -th quantile parameters to be estimated. To be simple, in this article we assume a linear dependency quantile structure. That is

$$Q_{\mathbf{Y}(t)|\mathbf{X}}(\tau, \mathbf{s}) = \mathbf{X}^T \boldsymbol{\beta}_\tau(\mathbf{s}, t), \quad (5)$$

where $\boldsymbol{\beta}_\tau(\mathbf{s}, t) = (\beta_{\tau 1}(\mathbf{s}, t), \dots, \beta_{\tau p}(\mathbf{s}, t))^T \in \mathbb{R}^p$ varies along t and also depends on the direction \mathbf{s} . In this article, we always fix a $\tau \in (0, 1)$ to estimate $\boldsymbol{\beta}_\tau(\mathbf{s}, t)$. Therefore, to simplify the notations we hereafter will drop the subscript τ if there is no confusion. The τ -th directional quantile envelope generated from the BQVCM (5) can be defined as in (3),

$$D(\tau, t) = \bigcap_{\mathbf{s} \in \mathcal{S}^1} H(\mathbf{s}, Q_{\mathbf{Y}(t)|\mathbf{X}}(\tau, \mathbf{s})), \quad (6)$$

where $D(\tau, t)$ depends on t and essentially constructs a bivariate quantile envelope tube along t for each fixed τ . Note that the quantile envelope tubes $D(\tau, t)$ are nested in terms of τ , as Tukey's depth contours (Tukey, 1975).

For given observations $\{\mathbf{y}_i(t_j), \mathbf{x}_i\}$, where $i = 1, \dots, n$ and $j = 1, \dots, J$. For $0 < \tau < 1$, to estimate $\boldsymbol{\beta}(\mathbf{s}, t)$ in (5), we minimize

$$\mathbf{L}(\mathbf{y}, \mathbf{x}, \mathbf{s}; \boldsymbol{\beta}(\mathbf{s})) = \sum_{i=1}^n \sum_{j=1}^J \rho_\tau(\mathbf{s}^T \mathbf{y}_i(t_j) - \mathbf{x}_i^T \boldsymbol{\beta}(\mathbf{s}, t_j)), \quad (7)$$

where ρ_τ is the quantile loss function defined in (1). Under certain conditions, the varying coefficients $\boldsymbol{\beta}(\mathbf{s}, t_j)$ can be well approximated by B-splines (Huang *et al.*, 2002, 2004). Let $\mathbf{H}(t) = (h_1(t), \dots, h_M(t))^T$ be the selected B-spline basis, where M is the total number of basis functions. The coefficients $\boldsymbol{\beta}(\mathbf{s}, t)$ are approximated by $\mathbf{C}(\mathbf{s})\mathbf{H}(t)$ with $\mathbf{C}(\mathbf{s})$ being a $p \times M$ coefficient matrix. Letting $\mathbf{B}(\mathbf{s})$ be the vectorization of $\mathbf{C}(\mathbf{s})$, i.e., a pM dimensional vector, then $\mathbf{C}(\mathbf{s})\mathbf{H}(t) = \mathbf{I}_p \otimes \mathbf{H}^T(t)\mathbf{B}(\mathbf{s})$. Then the loss function (7) is rewritten as

$$\mathbf{L}_b(\mathbf{y}, \mathbf{x}, \mathbf{s}; \mathbf{B}(\mathbf{s})) = \sum_{i=1}^n \sum_{j=1}^J \rho_\tau(\mathbf{s}^T \mathbf{y}_i(t_j) - \mathbf{x}_i^T \mathbf{I}_p \otimes \mathbf{H}^T(t_j)\mathbf{B}(\mathbf{s})). \quad (8)$$

In general, $\boldsymbol{\beta}(\mathbf{s}, t)$ is a smooth function of t ; see Zhu *et al.* (2012) and Zhou *et al.* (2015). To achieve the desired smoothness and also to avoid possible overfitting of the model, we impose an L_2 type penalty on $\boldsymbol{\beta}(\mathbf{s}, t)$,

$$\mathbf{P}_\lambda(\boldsymbol{\beta}(\mathbf{s}, t)) = \lambda \sum_{k=1}^p \int \left(\frac{\partial^2 \beta_k(\mathbf{s}, t)}{\partial t^2} \right)^2 dt, \quad (9)$$

where λ is the tuning parameter to control the smoothness of $\boldsymbol{\beta}(\mathbf{s}, t)$. The penalty in (9) can be written as

$$\mathbf{P}_\lambda(\boldsymbol{\beta}(\mathbf{s}, t)) = \mathbf{B}^T(\mathbf{s})\boldsymbol{\Omega}\mathbf{B}(\mathbf{s}), \quad (10)$$

where $\boldsymbol{\Omega} = \int (\partial^2 \mathbf{H}(t)/\partial t^2)^T (\partial^2 \mathbf{H}(t)/\partial t^2) dt$. Therefore, the penalized objective function of (7) is of the form

$$\mathbf{L}_{pb}(\mathbf{y}, \mathbf{x}, \mathbf{s}; \mathbf{B}(\mathbf{s})) = \mathbf{L}_b(\mathbf{y}, \mathbf{x}, \mathbf{s}; \mathbf{B}(\mathbf{s})) + \mathbf{B}^T(\mathbf{s})\boldsymbol{\Omega}\mathbf{B}(\mathbf{s}). \quad (11)$$

2.2 Multistage estimation procedure

In reality $\mathbf{B}(\mathbf{s})$ may be continuous or piecewise continuous in terms of direction \mathbf{s} . For example, in the case $\mathbf{Y}(t) = \mathbf{X}^T \boldsymbol{\beta}(t) + \boldsymbol{\epsilon}(t)$, where $\boldsymbol{\epsilon}(t)$ follows independent standard normal

distributions for all t , we have $\beta_\tau(\mathbf{s}, t) = \mathbf{s}^T \beta(t)$ for $\tau = .5$, which is a continuous function of the direction \mathbf{s} . To estimate $\mathbf{B}(\mathbf{s})$ using (11) for each individual direction \mathbf{s} without considering the correlations between different directions will lose efficiency and may not be able to capture the possible continuity of $\mathbf{B}(\mathbf{s})$. The problems could become more severe when the sample size is limited while many directions are considered. To improve the efficiency and warrant certain smoothness, we can estimate $\mathbf{B}(\mathbf{s})$ for all selected directions simultaneously. For example, a weighted loss function may be considered,

$$\sum_{r=1}^d L_{pb}(\mathbf{y}, \mathbf{x}, \mathbf{s}_r; \mathbf{B}(\mathbf{s}_r)) w(\mathbf{s}_r), \quad (12)$$

where $\mathbf{s}_r \in \mathbf{S} = \{\mathbf{s}_r : r = 1, \dots, d\}$ are selected directions and $w(\mathbf{s}_r)$ are weights to characterize the corrections of the loss functions at different directions. Similar strategies have been used in Bradic *et al.* (2011), Zhao and Xiao (2014) and others. However, the computational complexity raised in (12) by simultaneously considering possibly hundreds of directions may be beyond the limit of the current computational capacity. This can be seen more clearly by noticing that the dimension of $\{\mathbf{B}(\mathbf{s}_r) : \mathbf{s}_r \in \mathbf{S}\}$ is of dpM , where both d and M are in the magnitude of hundreds. To estimate parameters of such high dimensions, the inverse of large matrices will be involved. Unless there is certain particular structure in the matrices, in general the inverses will be computationally difficult or even impossible.

In this section, we propose a multistage estimation procedure based on the propagation-separation (PS) approach (Polzehl and Spokoiny, 2000, 2006) to gradually borrow information from nearby directions with increasing number of directions. The PS method is capable of handling the computational complexity raised by simultaneously considering multiple directions to efficiently estimate varying coefficients while guaranteeing certain smoothness along directions. To the best of our knowledges, this is the first method to construct the directional quantile regression envelopes by simultaneously considering multiple directions. Our multistage estimation procedure includes three main stages, namely, *Stage I: initialization*, *Stage II: adaptive updating*, and *Stage III: stop checking*. We first briefly describe the three stages in the following.

Stage I: initialization. Use (11) to obtain the initial estimates for $\mathbf{B}(\mathbf{s}_r)$, denoted by

$\hat{\mathbf{B}}_0(\mathbf{s}_r)$ for each individual direction $\mathbf{s}_r \in \mathcal{S}$.

Stage II: adaptive updating. Use PS to adaptively update $\hat{\mathbf{B}}_{c-1}(\mathbf{s}_r)$ from the $c - 1$ step for each direction in \mathcal{S} by gradually increasing the number of nearby directions.

Stage III: stop checking. Calculate the stopping criterion for the updated $\hat{\mathbf{B}}_c(\mathbf{s}_r)$ and determine if the updating needs stop.

The multistage estimation procedure will iterate between *Stage II* and *Stage III* until stop or the maximum number of iteration is reached. By gradually increasing the number of nearby directions and adaptively updating, the coefficients $\mathbf{B}(\mathbf{s}_r)$ can be efficiently estimated with certain smoothness while the computation can be largely reduced.

In *Stage I: initialization*, to minimize (11), it is a convex optimization problem with a nonsmooth quantile loss function and an L_2 type penalty in the objective function, which can be reformulated and effectively solved by ADMM (Boyd *et al.*, 2011) as shown in the next Section. The minimization of a nonsmooth quantile loss plus an L_2 penalty is a recurring theme in our multistage estimation procedure. In *Stage II*, the optimization is essentially the same minimization, which will be shown next. Thanks to the computational efficiency of ADMM, our multistage estimation procedure can adaptively update the coefficients effectively.

In *Stage II: adaptive updating*, to adaptively update the estimates of $\mathbf{B}(\mathbf{s}_r)$, we first define a nearby direction set sequence. For simplicity, we assume the directions $\mathcal{S} = \{\mathbf{s}_r : r = 1, \dots, d\}$ are equally distributed in \mathcal{S}^1 and denote the distance by d_0 . Given a direction $\mathbf{s}_{r_0} \in \mathcal{S}$, we define a nearby direction set sequence $\{R_c(\mathbf{s}_{r_0})\}_{c=1}^C$ through a nondecreasing bandwidth sequence $\{h^c\}_{c=1}^C$, where C is the preselected maximum steps of iteration. In particular, $R_c(\mathbf{s}_{r_0}) = \{\mathbf{s}_r : \|\mathbf{s}_r - \mathbf{s}_{r_0}\| \leq d_0 h^c, \mathbf{s}_r \in \mathcal{S}\}$, where $\|\cdot\|$ denotes the L_2 norm. In this article, we choose $d = 100$, $h = 1.15$ and $C = 5$. For fixed \mathbf{s}_{r_0} , in each iteration we update the estimates by minimizing the following loss function

$$\begin{aligned} & L_{wpb}^c(\mathbf{y}, \mathbf{x}, \mathbf{s}_{r_0}; \mathbf{B}(\mathbf{s}_{r_0})) \\ &= \sum_{\mathbf{s}_r \in R_c(\mathbf{s}_{r_0})} w \left(\hat{\mathbf{B}}_{c-1}(\mathbf{s}_{r_0}), \mathbf{s}_r \right) L_b(\mathbf{y}, \mathbf{x}, \mathbf{s}_r; \mathbf{B}(\mathbf{s}_{r_0})) + \mathbf{B}^T(\mathbf{s}_{r_0}) \Omega \mathbf{B}(\mathbf{s}_{r_0}), \end{aligned} \quad (13)$$

where $\hat{\mathbf{B}}_{c-1}(\mathbf{s}_{r_0})$ are the estimates from the $c - 1$ step and $w\left(\hat{\mathbf{B}}_{c-1}(\mathbf{s}_{r_0}), \mathbf{s}_r\right)$ are weights that determine the amount of information borrowed from nearby directions. Plugging the equation (8), it can be seen that (13) is also a nonsmooth quantile loss plus an L_2 penalty, which can be solved by ADMM.

The weight function $w\left(\hat{\mathbf{B}}_{c-1}(\mathbf{s}_{r_0}), \mathbf{s}_r\right)$ depends on two quantities: the distance between the directions \mathbf{s}_{r_0} and \mathbf{s}_r and the similarity between $\hat{\mathbf{B}}_{c-1}(\mathbf{s}_{r_0})$ and $\hat{\mathbf{B}}_{c-1}(\mathbf{s}_r)$. Let

$$D\left(\hat{\mathbf{B}}(\mathbf{s}_{r_0}), \hat{\mathbf{B}}(\mathbf{s}_r)\right) = \left(\hat{\mathbf{B}}(\mathbf{s}_{r_0}) - \hat{\mathbf{B}}(\mathbf{s}_r)\right)^T \hat{\Sigma}^{-1}\left(\hat{\mathbf{B}}(\mathbf{s}_{r_0})\right) \left(\hat{\mathbf{B}}(\mathbf{s}_{r_0}) - \hat{\mathbf{B}}(\mathbf{s}_r)\right), \quad (14)$$

where $\hat{\Sigma}\left(\hat{\mathbf{B}}(\mathbf{s}_{r_0})\right)$ is the estimated covariance matrix of $\hat{\mathbf{B}}(\mathbf{s}_{r_0})$. The weight function is of the form

$$w\left(\hat{\mathbf{B}}_{c-1}(\mathbf{s}_{r_0}), \mathbf{s}_r\right) = K_{loc}\left(\|\mathbf{s}_r - \mathbf{s}_{r_0}\|/(d_0 h^c)\right) K_{st}\left(D\left(\hat{\mathbf{B}}_{c-1}(\mathbf{s}_{r_0}), \hat{\mathbf{B}}_{c-1}(\mathbf{s}_r)\right)/C_n\right), \quad (15)$$

where both K_{loc} and K_{st} are nonnegative kernel function with compact support and C_n is a tuning parameter depending on n . In this article, we choose $C_n = n^\alpha \chi_1^2(.8)$, $\alpha \in [.3, 1.3]$ as suggested in Li *et al.* (2011); Zhu *et al.* (2014). The kernel function K_{loc} gives less weight to those directions far from \mathbf{s}_{r_0} . The kernel K_{st} downweights the directions \mathbf{s}_r which has large $D\left(\hat{\mathbf{B}}(\mathbf{s}_{r_0}), \hat{\mathbf{B}}(\mathbf{s}_r)\right)$. We choose $K_{loc}(u) = (1 - u)_+$ and $K_{st}(u) = \min(1, 2(1 - u)_+)$ in our simulations and real data analysis. For other available kernel functions, see Polzehl and Spokoiny (2000, 2006), Li *et al.* (2011), Zhu *et al.* (2014).

In *Stage III: stop checking*, we start to check the stopping criterion after a few iterations of *Stage II*, say, c_0 iterations. The stopping criterion is based on a normalized distance between $\hat{\mathbf{B}}_c(\mathbf{s}_r)$ and $\hat{\mathbf{B}}_{c_0}(\mathbf{s}_r)$, that is

$$D\left(\hat{\mathbf{B}}_c(\mathbf{s}_r), \hat{\mathbf{B}}_{c_0}(\mathbf{s}_r)\right) = \left(\hat{\mathbf{B}}_c(\mathbf{s}_r) - \hat{\mathbf{B}}_{c_0}(\mathbf{s}_r)\right)^T \hat{\Sigma}^{-1}\left(\hat{\mathbf{B}}_{c_0}(\mathbf{s}_r)\right) \left(\hat{\mathbf{B}}_c(\mathbf{s}_r) - \hat{\mathbf{B}}_{c_0}(\mathbf{s}_r)\right). \quad (16)$$

The iteration stops if $\hat{\mathbf{B}}_c(\mathbf{s}_r)$ falls outside the ellipsoid $\{\hat{\mathbf{B}}_c(\mathbf{s}_r) : D\left(\hat{\mathbf{B}}_c(\mathbf{s}_r), \hat{\mathbf{B}}_{c_0}(\mathbf{s}_r)\right) \leq C_s\}$, where C_s is a preselected constant, say $C_s = \chi_q^2(.8/c)$, where $q = dpM$ is the dimension of $\hat{\mathbf{B}}_c(\mathbf{s}_r)$; see Li *et al.* (2011); Zhu *et al.* (2014). If $\hat{\mathbf{B}}_c(\mathbf{s}_r)$ is lying within the ellipsoid, we set $c = c + 1$ and continue *Stage II* to update it in the direction \mathbf{s} . In general, the initial estimates are consistent, so the updated smoothing estimates shall not be too far away from the initial ones. An alternative stopping criterion is to check each individual

component of $\hat{\mathbf{B}}_c(\mathbf{s}_r)$. Let

$$d\left(\hat{B}_c^k(\mathbf{s}_r), \hat{B}_{c_0}^k(\mathbf{s}_r)\right) = \left(\hat{B}_c^k(\mathbf{s}_r) - \hat{B}_{c_0}^k(\mathbf{s}_r)\right)^2 \hat{\sigma}^{-2}\left(\hat{B}_{c_0}^k(\mathbf{s}_r)\right), \quad (17)$$

where $\hat{B}_{c_0}^k(\mathbf{s}_r)$ is a component of $\hat{\mathbf{B}}_c(\mathbf{s}_r)$ and $\hat{\sigma}^2\left(\hat{B}_{c_0}^k(\mathbf{s}_r)\right)$ is the estimated variance of $\hat{B}_{c_0}^k(\mathbf{s}_r)$. The iteration stops if any $d\left(\hat{B}_c^k(\mathbf{s}_r), \hat{B}_{c_0}^k(\mathbf{s}_r)\right) > \chi_1^2(.8/c)$; otherwise we set $c = c+1$ and continue the *Stage II*. Our simulation studies show that the latter works slightly better; so we choose to use the individual criterion in this article.

2.3 ADMM Algorithm

The optimization problems in equations (11) and (13) are convex, which can be solved by many generic convex optimization techniques, for example, the simplex method (Koenker, 2005) and the interior point method (Koenker and Park, 1996). However, these methods do not take advantage of the special structure of (11) and (13), that is, both can be split into two sub-convex optimization problems: a nonsmooth quantile loss function plus an L_2 type penalty. A more efficient algorithm to solve our convex optimization problems is the alternating direction method of multipliers (ADMM). The ADMM algorithm was developed in the 1970s with roots in the 1950s (Hestenes, 1969; Gabay and Mercier, 1976), and received renewed interest due to that it is efficient to tackle large scale problems and can solve optimization problems with multiple nonsmooth terms in the objective function (Boyd *et al.*, 2011; Lin *et al.*, 2013). ADMM is a powerful algorithm for convex problems that can be decomposed into several sub-convex problems (Boyd *et al.*, 2011). In this section, we reformulate our optimization problems of (11) and (13) and derive their ADMM algorithms based on the observation that they can be split into two sub-convex optimization problems and one of the sub-problems has a nonsmooth function.

Let $f(x)$ and $g(z)$ be convex functions of two vectors x and z , respectively. Suppose A and B are two unknown matrices and c is a known vector. We have the following convex optimization problem with constraints,

$$\begin{aligned} \text{minimize} \quad & f(x) + g(z) \\ \text{s.t.} \quad & Ax + Bz = c, \end{aligned} \quad (18)$$

which can be easily solved by ADMM. The augmented Lagrangian function (Powell, 1967; Hestenes, 1969) of (18) can be written as

$$L_\rho(x, z, y) = f(x) + g(z) + y^T(Ax + Bz - c) + (\rho/2)\|Ax + Bz - c\|^2, \quad (19)$$

where $\|\cdot\|$ is the L_2 norm and ρ is a tuning parameter, which is chosen to be 1.2 in this article (Boyd *et al.*, 2011). Letting $u = (1/\rho)y$ and $u_k = (1/\rho)y^k$, the scaled augmented Lagrangian function is of the form

$$L_{s\rho}(x, z, y) = f(x) + g(z) + (\rho/2)\|Ax + Bz - c + u\|^2 - (\rho/2)u_2. \quad (20)$$

The ADMM algorithm finds the optimal solution of (20) by iterating through the following three steps:

$$\begin{aligned} x^{k+1} &= \operatorname{argmin}_x (f(x) + (\rho/2)\|Ax + Bz^k - c + u^k\|^2), \\ z^{k+1} &= \operatorname{argmin}_z (g(z) + (\rho/2)\|Ax^{k+1} + Bz - c + u^k\|^2), \\ u^{k+1} &= u^k + (Ax^{k+1} + Bz^{k+1} - c). \end{aligned} \quad (21)$$

Note the formulas are in the scaled form of ADMM which is often shorter and more convenient to solve than in the unscaled form, so we will use the scaled form in this article. Step one optimizes over x and step two optimizes over z . In the last step, it brings x and z together to match the constraints. The key requirement for (18) is that x and z do not share common elements. In general, steps one and two in (21) admit simple forms, which will be illustrated later in our proposed method; for more examples, see Boyd *et al.* (2011).

Both (11) and (13) can be written as the sum of a nonsmooth quantile loss function and an L_2 type penalty. That is,

$$\rho_\tau(y - Xb) + \lambda b^T \Omega b, \quad (22)$$

where ρ_τ is the quantile loss, y is a known vector, X and Ω are known matrices, λ is the tuning parameter and b is the vector we optimize over. To adapt to the ADMM algorithm, we reformulate (22) to

$$\begin{aligned} \text{minimize} \quad & \rho_\tau(r) + \lambda b^T \Omega b, \\ \text{s.t.} \quad & r + Xb = y. \end{aligned} \quad (23)$$

Observing that $f(r) = \rho_\tau(r)$, $g(b) = \lambda b^T \Omega b$, $A = I$, $B = X$, and $c = y$ comparing with (18), similar to (21) we solve (23) by iterating the following

$$\begin{aligned} r^{k+1} &= \operatorname{argmin}_r (\rho_\tau(r) + (\rho/2) \|r + Xb^k - y + u^k\|^2), \\ b^{k+1} &= \operatorname{argmin}_b (\lambda b^T \Omega b + (\rho/2) \|r^{k+1} + Xb - y + u^k\|^2), \\ u^{k+1} &= u^k + (r^{k+1} + Xb^{k+1} - y). \end{aligned} \quad (24)$$

The first step in (24) can be simplified by the soft-thresholding operator. That is, step one has the following closed form,

$$r^{k+1} = S_{1/(2\rho)} (u^k - y + Xb^k - (2\tau - 1)/(2\rho)), \quad (25)$$

where $S_a(v) = (v - a)_+ - (-v - a)_+$ is a soft-thresholding operator. The second step is a least square loss plus an L_2 type penalty and admits the following ridge regression type closed form,

$$b^{k+1} = (2\lambda\Omega/\rho + X^T X)^{-1} X^T (y - r^{k+1} + u^k). \quad (26)$$

Note that the inverse of $2\lambda\Omega/\rho + X^T X$ only needs to be calculated once. Therefore, the iterations in (23) are very fast and efficient.

We use the termination criterion suggested by Boyd *et al.* (2011), which is based on primal residuals r_{pri} and dual residuals r_{dual} . At the k -th iteration, the primal residuals r_{pri}^k and dual residuals r_{dual}^k are calculated according to

$$\begin{aligned} r_{pri}^k &= y - Xb^k - r^k, \\ r_{dual}^k &= \rho X(b^k - b^{k-1}), \end{aligned} \quad (27)$$

respectively. The termination criterion is

$$\|r_{pri}^k\| \leq \epsilon^{pri} \text{ and } \|r_{dual}^k\| \leq \epsilon^{dual}, \quad (28)$$

where $\epsilon^{pri} > 0$ and $\epsilon^{dual} > 0$ are feasibility tolerances for the primal and dual feasibility conditions. These tolerances can be chosen using an absolute and relative tolerances (Boyd *et al.*, 2011),

$$\begin{aligned} \epsilon^{pri} &= \sqrt{p}\epsilon^{abs} + \epsilon^{rel} \max (\|r^k\|_2, \|Xb^k\|, \|y\|), \\ \epsilon^{dual} &= \sqrt{n}\epsilon^{abs} + \epsilon^{rel} \|u^k\|, \end{aligned} \quad (29)$$

where $\epsilon^{abs} > 0$ and $\epsilon^{rel} > 0$ are absolute and relative tolerance, respectively. The absolute tolerance and relative tolerance can be any small numbers in practical calculations. For example, we choose $\epsilon^{abs} = 10^{-4}$ and $\epsilon^{rel} = 10^{-2}$ in this article.

3 Numerical Studies

3.1 Simulation Studies

In this section, we conduct simulation studies to evaluate the performance of our proposed methods. We investigate models of different types of coefficients and various error distributions. Let $\mathbf{Y}(t) = (Y_1(t), Y_2(t))^T \in \mathbb{R}^2$ be a bivariate functional response at time t , where $t \in [0, 1]$, $\mathbf{X} \in \mathbb{R}^3$ be the covariates of interest such that $\mathbf{X} = (1, X_1, X_2)^T$; and they have the following relationship,

$$\mathbf{Y}(t) = (\mathbf{X}^T \boldsymbol{\beta}_1(t), \mathbf{X}^T \boldsymbol{\beta}_2(t))^T + \boldsymbol{\epsilon}(t), \quad (30)$$

where $\boldsymbol{\beta}_i(t) = (\beta_{i0}(t), \beta_{i1}(t), \beta_{2i}(t))^T$, for $i = 1$ and 2 . In our simulation studies, we set $X_1 \sim \text{Bernoulli}(.5)$, and $X_2 \sim \text{Uniform}(0, 1)$, where the choice of two variables is motivated by our DTI data in Section 3.2. In general, X_1 and X_2 represent binary (e.g. gender or diagonal status) and scaled continuous variables (e.g. age, or height). Two types of varying coefficients $\boldsymbol{\beta}(t)$ are considered, smooth and rough, which are

$$\begin{aligned} \boldsymbol{\beta}_1(t) &= (2t + 1, \sin(t) + 2, \cos(t) - 2)^T, \\ \boldsymbol{\beta}_2(t) &= (2t - 1, \cos(t) - 2, \sin(t) + 3)^T, \end{aligned} \quad (31)$$

and

$$\begin{aligned} \boldsymbol{\beta}_1(t) &= (40t/(2t + 1), (t^2 + 3)/(t - 2), t + 3)^T, \\ \boldsymbol{\beta}_2(t) &= (\log(t + 1), t + 1, 3t^2 - 2)^T, \end{aligned} \quad (32)$$

respectively. Furthermore, we consider three types of error distributions, namely, normal, t , and χ^2 distributions. In particular, the three error distributions are

(I) a bivariate normal distribution

$$\boldsymbol{\epsilon}(t) \sim N(\boldsymbol{\mu}, \Sigma), \quad (33)$$

where $\boldsymbol{\mu} = (0, 0)^T$ and $\Sigma = \text{diag}(.8, .8)$;

(II) a bivariate t distribution with degrees of freedom 3

$$\boldsymbol{\epsilon}(t) \sim t_3(\boldsymbol{\mu}, \Sigma), \quad (34)$$

where $\boldsymbol{\mu} = (0, 0)^T$ and $\Sigma = \text{diag}(.8^5, .8^5)$; and

(III) a bivariate χ^2 distribution with degrees of freedom 3

$$\boldsymbol{\epsilon}(t) \sim .8 (a_1^2 + a_2^2 + a_3^2, a_3^2 + a_4^2 + a_5^2)^T, \quad (35)$$

where $a_i \sim N(0, 1)$ for $i = 1, \dots, 5$ are mutually independent.

The first error distribution is very common; the second distribution mimics heavy tailed distributions and the last one stands for skewed and correlated distributions. We carefully choose the parameters of the error distributions so that the models have comparable signal-to-noise ratios (SNRs).

We choose $J = 50$ equally spaced points t from the interval $[0, 1]$ and the sample size of our Monte Carlo simulations is set to be 200. Then we estimate the coefficients using our proposed methods in Section 2.2. In particular, we choose 100 evenly spaced directions in $[-\pi, \pi]$ and B-spline basis with 14 evenly spaced knots in $[.02, .93]$. The ADMM algorithms in Section 2.3 are implemented in R with core parts written in C. Then we construct the $\tau = \{.05, .1, .2\}$ -th directional quantile envelopes according to (6); for detailed construction algorithms, see Kong (2009); Hallin *et al.* (2010), and Kong and Mizera (2012). To evaluate the resulting directional envelopes, we look at two measures, namely, the envelope curvature — the average change rate of slope of the envelope, and the coverage rate — the proportion of data points covered by the envelope, denoted by κ and ν , respectively. We repeat our Monte Carlo simulations 100 times and calculate the mean and standard deviation of κ and ν of the 100 replications from the initial and updated estimates. The initial varying coefficients are calculated by (11) and the updated ones are estimated by our multistage estimation procedure.

We present the results in Table 1 for a selected data point with $X_1 = 1, X_2 = .5$ at $t = .7$, where the true κ and ν values are calculated from the direction quantile envelopes

Table 1: The envelope curvatures κ and coverage rates ν of the true, initial, and updated directional quantile envelopes at quantile levels $\tau = \{.05, .1, .2\}$ for simulated models with smooth (S) or rough (R) coefficients and different error distributions, I, II, and III. The standard deviations of the initial and updated κ and ν are listed in the brackets.

| | | | $\tau=.05$ | | | $\tau=.1$ | | | $\tau=.2$ | | |
|---|-----|----------|------------|------------|------------|-----------|------------|------------|-----------|------------|------------|
| | | | True | Initial | Updated | True | Initial | Updated | True | Initial | Updated |
| S | I | κ | .80 | 3.0(2.2) | 1.5(.9) | 1.08 | 4.28(3.9) | 1.78(.9) | 2.63 | 6.03(3.8) | 4.13(2.1) |
| | | ν | .740 | .742(.024) | .741(.013) | .560 | .589(.020) | .575(.020) | .295 | .298(.017) | .295(.016) |
| | II | κ | 1.37 | 2.97(2.0) | 2.27(2.0) | 2.02 | 4.0(2.0) | 2.82(2.2) | 2.34 | 9.94(10.2) | 6.54(4.4) |
| | | ν | .790 | .768(.026) | .776(.013) | .620 | .623(.023) | .621(.023) | .340 | .328(.020) | .340(.018) |
| | III | κ | .56 | .65(1.2) | .64(.9) | 1.23 | 2.43(1.9) | 2.03(1.8) | 1.86 | 3.56(2.0) | 2.76(1.3) |
| | | ν | .723 | .614(.017) | .722(.019) | .540 | .512(.022) | .551(.018) | .280 | .312(.015) | .287(.014) |
| R | I | κ | .97 | 2.77(2.5) | 2.17(1.7) | 2.66 | 4.68(2.4) | 2.72(2.1) | 3.29 | 6.19(5.5) | 3.79(2.9) |
| | | ν | .740 | .802(.022) | .740(.016) | .560 | .600(.025) | .533(.021) | .295 | .301(.018) | .293(.017) |
| | II | κ | 1.52 | 2.82(1.8) | 1.53(.9) | 1.50 | 4.10(2.7) | 4.00(1.8) | 2.96 | 6.86(3.6) | 5.06(3.3) |
| | | ν | .790 | .809(.019) | .792(.010) | .620 | .628(.024) | .626(.018) | .340 | .312(.018) | .333(.017) |
| | III | κ | .90 | 1.10(1.5) | 1.60(1.5) | 1.01 | 1.71(1.2) | 1.71(1.1) | 3.17 | 3.97(3.1) | 3.18(2.2) |
| | | ν | .720 | .682(.022) | .719(.017) | .540 | .583(.019) | .570(.018) | .280 | .317(.014) | .284(.013) |

from 5000 generated observations at the selected point in our simulation models. For the models with smooth coefficients, Table 1 shows that the envelope curvature κ values for the updated quantile envelopes are closer to the true values compared with the initial ones at all the three selected quantile levels. Moreover, the updated κ values have smaller standard deviations than the initial ones, which are shown in the bracket in Table 1. Similar patterns are observed for the models with rough coefficients in Table 1, some patterns are weaker or slightly reversing though. These indicate that our proposed multistage estimation procedure is capable of obtaining quantile envelopes with desired smoothness and smaller variations. In Table 1, for both smooth and rough coefficients we observe that the updated coverage rate ν values have much smaller bias compared with the initial estimates and in general have smaller or comparable standard deviations, shown in the bracket in Table 1.

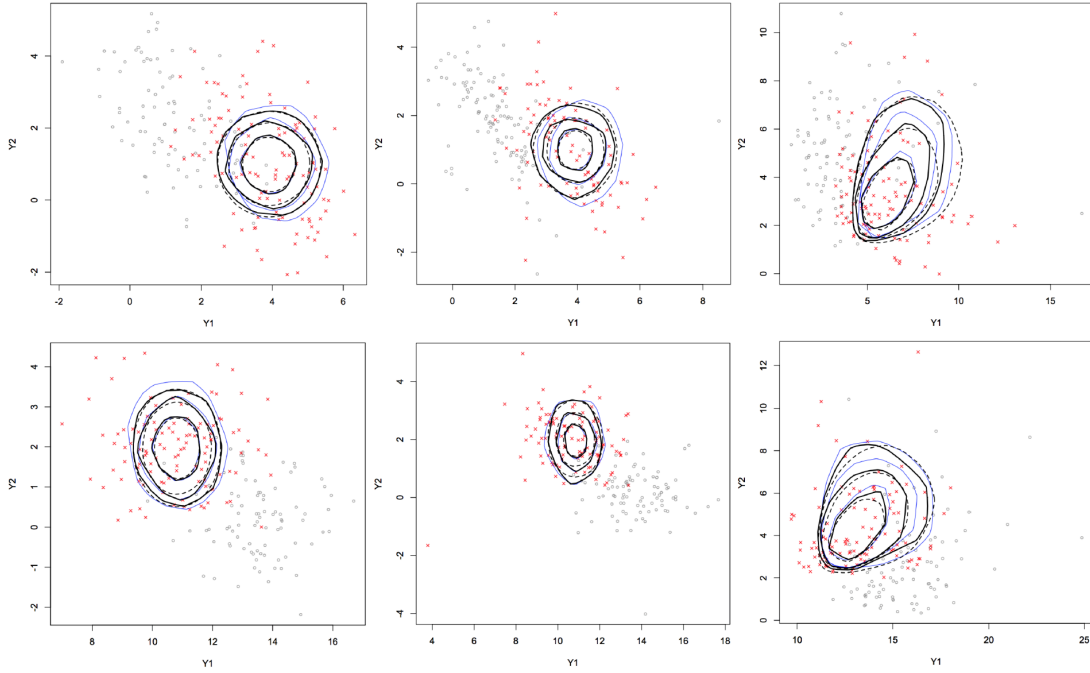


Figure 1: One selected data set at $X_1 = 0$ (grey circle) or $X_1 = 1$ (red cross), $X_2 = .5$, and around $t = .7$ overlaid the true (thick dashed dark), initial (thin solid blue), and the updated (thick solid dark) directional envelopes at the data point $(X_1, X_2, t) = (1, .5, .7)$ from the models with smooth (upper panels) or rough (lower panels) coefficients and three error distributions I (left panels), II (middle panels), and III (right panels).

Therefore, our multistage estimation procedure is able to substantially reduce the bias of the coverage rate ν by adaptively updating our estimates through borrowing information from nearby directions. This implies that the adopted PS method is effective in parameter estimation (and thus predicting data points), as it improves not only the smoothness but also the accuracy of the regression coefficients. In Figure 1, the true (thick dashed dark), initial (thin solid blue), and the updated (thick solid dark) directional envelopes at the selected data point further confirm our observations that the updated envelopes are closer to the true ones and smoother than the initial ones. In summary, our proposed multistage estimation procedure is more efficient in constructing directional quantile envelopes. Moreover, it provides quantile envelopes with not only desired smoothness but also more accurate coverage rates.

We conclude this section with some comments on the choice of parameters in the multistage estimation procedure, which is crucial when applying this method, especially in the PS method. One key parameter is the scale parameter C_n in the kernel function K_{st} to penalize the dissimilarity between two directions in a manner similar to bandwidth in local polynomial smoothing (Fan and Gijbels, 1996). Based on our experience, we recommend $C = n^\alpha \chi_1^2(0.8)$, where $\alpha \in [0.3, 1.3]$, n is the sample size and $\chi_1^2(u)$ is the u -th upper quantile of the chi-square distribution with 1 degree of freedom (Li *et al.*, 2011; Zhu *et al.*, 2014). When α increases, K_{st} increases and more information of the nearby directions is included. Another important parameter is the penalty parameter λ that controls the smoothness along t — if λ is small, less smoothness is imposed; otherwise, more smoothness is imposed. We suggest choose λ from $\{0.001, 0.01, 0.1, 1\}$. Although cross-validation can always be used to choose λ , we only do that in the initial stage for each quantile level and in the following update stages we choose the same λ to save computation time.

3.2 Neuroimaging data analysis

The data set consists of 128 healthy full-term infants (75 males and 53 females) from a clinical study on early brain development, which was approved by the Institutional Review Board of the University of North Carolina at Chapel Hill. The mean gestational age at MR scanning of the 128 infants was 298 ± 17.6 days. For each subject, the DTI images were obtained by using a single shot EPI DTI sequence (TR/TE=5400/73 msec) with eddy current compensation. The six non-collinear directions were applied at the b -value of 1000 s/mm^2 with a reference scan ($b = 0$). The voxel resolution was isotropic 2 mm, and the in-plane field of view was set at 256 mm in both directions. To improve the signal-to-noise ratio of the images, a total of five scans were acquired and averaged.

To construct the diffusion tensors, there are two key steps including a weighted least squares estimation method (Zhu *et al.*, 2007) and a DTI atlas building process followed by an atlas-based tractography procedure; for more details see Zhu *et al.* (2011). In this article, we focus on the fiber bundle of the genu of the corpus callosum (GCC), shown in the left panel of Figure 2, which is an area of white matter in the brain. Two diffusion properties, standardized fractional anisotropy (FA) and standardized mean diffusivity (MD),

are to be studied; They are bivariate functional responses of arclength observed in 45 grid points, shown in the middle (FA along GCC - GFA) and right panels (MD along GCC - GMD) of Figure 2. FA and MD, respectively, measure the inhomogeneous extent of local barriers to water diffusion and the averaged magnitude of local water diffusion.

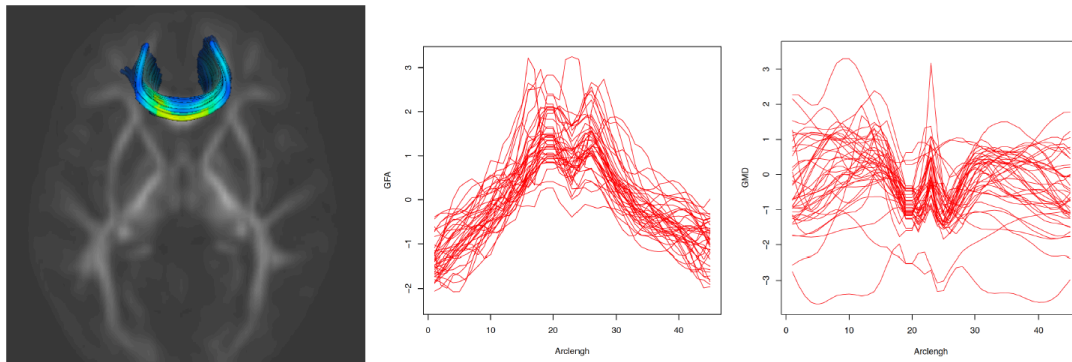


Figure 2: Genu tract (left panel) and two diffusion properties, fractional anisotropy (GFA) (middle panel) and mean diffusivity (GMD) (right panel), observed in 45 grid points along the genu tract from 40 randomly selected infants.

In this analysis, our aim is to study the quantile association between two diffusion properties (FA and MD) and a set of covariates. In particular, we fit model (5), where $\mathbf{Y} = (\text{GFA}, \text{GMD})^T$ — the standardized GFA and GMD values and $\mathbf{x}_i = (1, \text{Gender})$, G with G standing for the gestational age. After finding the directional quantile coefficients at quantile levels $\tau = \{.05, .1, .2, .3\}$ using 100 selected directions, we construct the corresponding directional quantile envelopes by (6). We chose 100 directions because previous studies have shown that 100 directions are sufficient to characterize the envelopes (Kong, 2009; Kong and Mizera, 2012). Using the directional quantile envelopes, our analysis provides new insights on the early brain development at both population and individual levels.

To illustrate the information on population level we can obtain from the resulting envelopes, we look at the quantile envelopes of GFA and GMD at gestational age 300 for males (upper panels) and females (lower panels) at three different arclengths, 10 (left panels), 20 (middle panels) and 30 (right panels), separately; see Figure 3. We observe similar patterns for males and females in terms of shape and location of the quantile envelopes

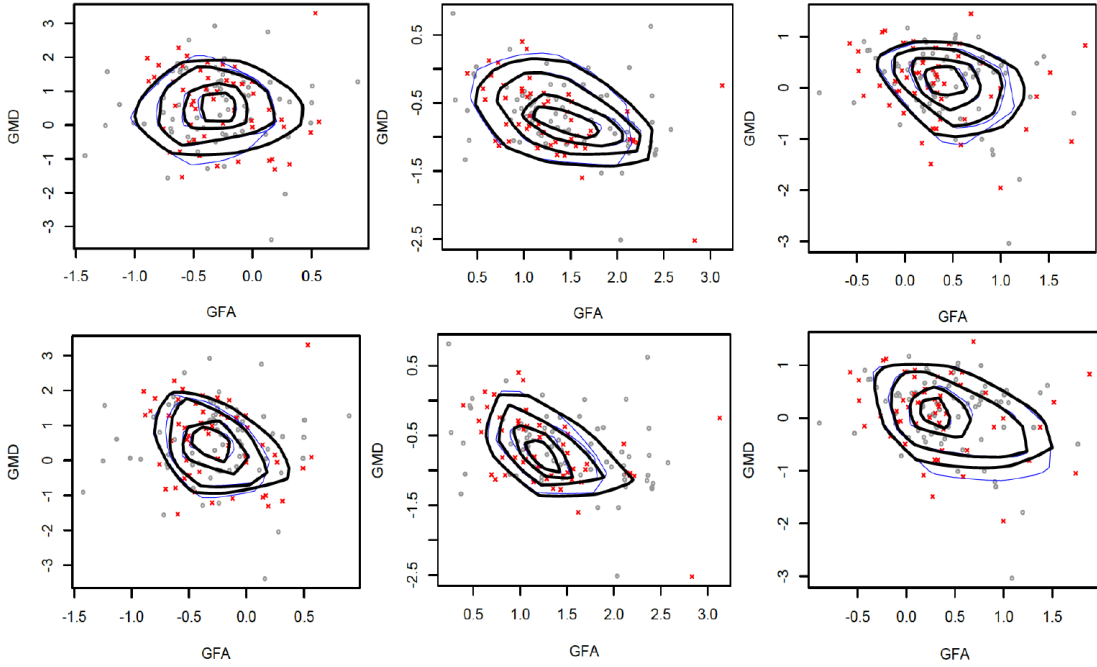


Figure 3: Quantile envelopes of GFA and GMD at gestational age 300 for males (upper panels) and females (lower panels) at three different arclengths, 10 (left panels), 20 (middle panels) and 30 (right panels) overlaid on the observed data points (males - grey circle, females - red cross). The quantile levels from outer to inner envelopes are $\tau = \{.05, .1, .2, .3\}$ and the thin blue and thick dark envelopes are initial and updated envelopes, respectively.

at different arclengths. On the other hand, we also observe some differences; for example, the envelope sizes for males are bigger at arclengths 10 and 30 while smaller at arclength 20 than those for females. The envelope shapes and locations change with arclength for both males and females; for instance, the ranges of the 95 percent quantile envelope of males are $GMD \in (-1, 2)$ and $GFA \in (-1, 0.5)$ at arclength 10, $GMD \in (-1.5, 0.25)$ and $GFA \in (0.5, 2.5)$ at arclength 20, and $GMD \in (-1, 1)$ and $GFA \in (-0.25, 1.25)$ at arclength 30. The 90 and 95 initial quantile envelopes for males are crossing with each other while the updated ones are not by borrow information from nearby directions (upper middle panel in Figure 3). This indicates that our method can effectively use the information in the data to yield more harmonious model structures.

In Figure 4, we display quantile envelopes of GFA and GMD at arclength 30 for males (upper panels) and females (lower panels) at three different gestational ages, 280 (left panels), 300 (middle panels) and 340 (right panels). The quantile envelopes show consistent patterns for males and females in terms of shape and location. The quantile envelope sizes increase with gestational ages for both males and females; the sizes for males are smaller than those for females though. As gestational age increases, the joint distributions of GFA and GMD become more skewed to the lower right corner (right panels in Figure 4) as evidenced by the shapes of the quantile envelopes and the distances between them.

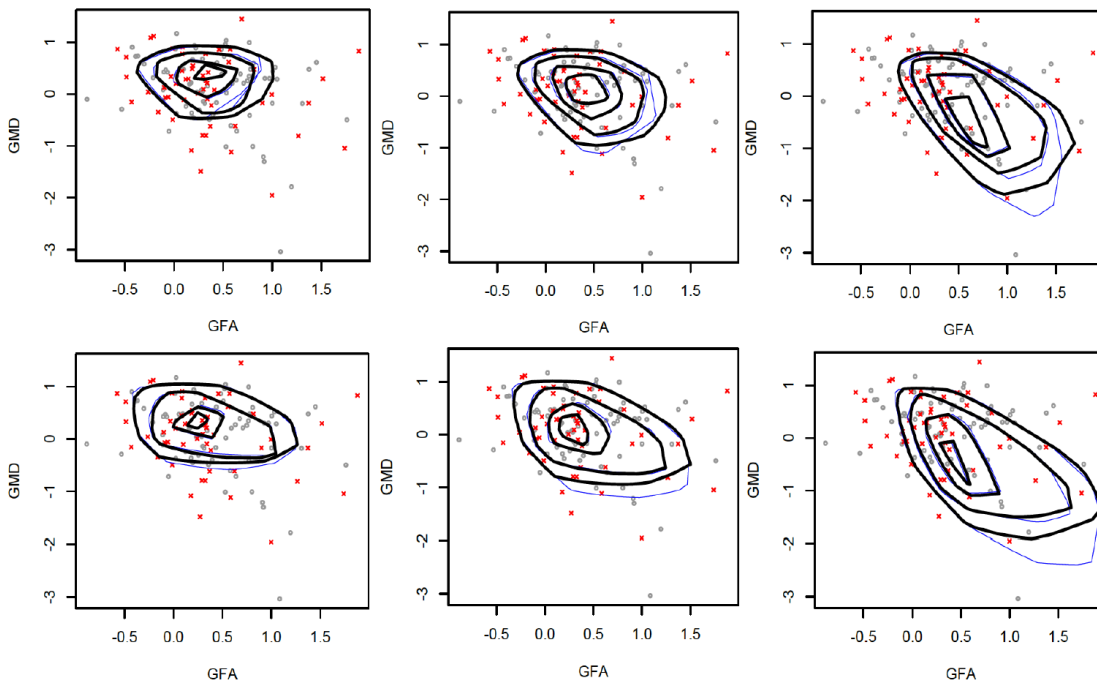


Figure 4: Quantile envelopes of GFA and GMD at arclength 30 for male (upper panels) and female (lower panels) at three different gestational ages, 280 (left panels), 300 (middle panels) and 340 (right panels) overlaid on the observed data points (male - grey circle, female - red cross). The quantile levels from outer to inner envelopes are $\tau = \{.05, .1, .2, .3\}$ and the thin blue and thick dark envelopes are initial and updated envelopes, respectively.

In the end, we demonstrate how to use the directional quantile envelopes at individual levels to gain insights to early brain development. For this purpose, we display in Figure 5 the quantile envelopes of GFA and GMD at arclength 30 for females at gestational age

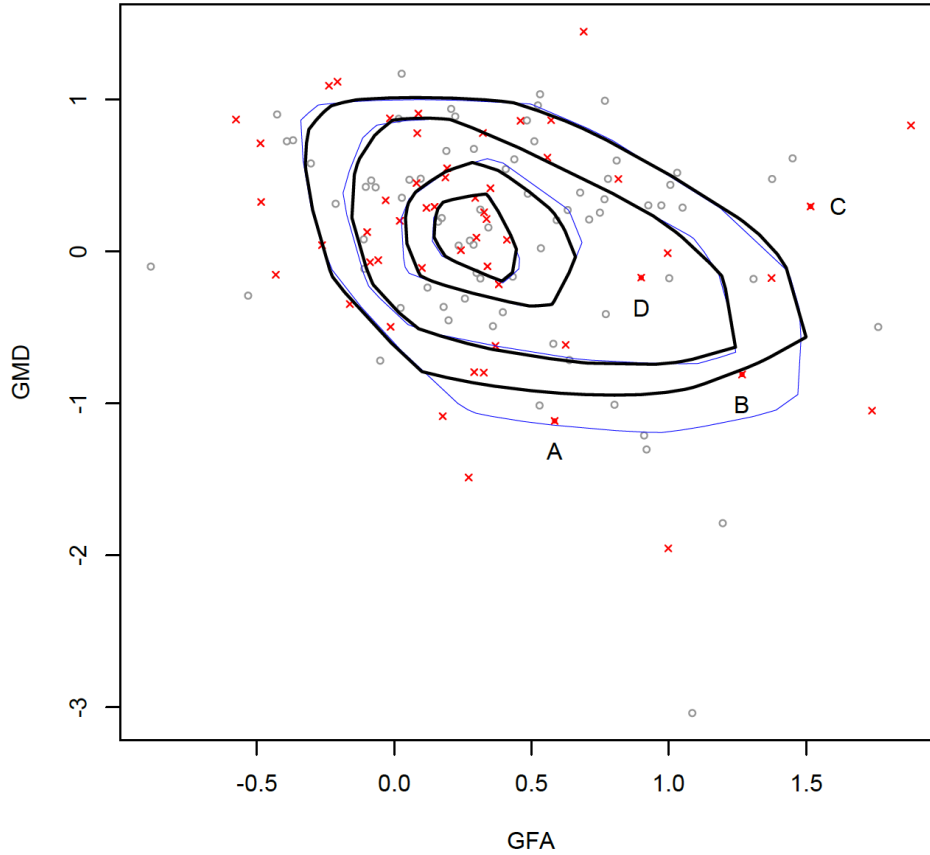


Figure 5: Quantile envelopes of GFA and GMD at arclength 30 for females at gestational age 300 overlaid on the observed data points (male - grey circle, female - red cross). The quantile levels from outer to inner envelopes are $\tau = \{.05, .1, .2, .3\}$ and the thin blue and thick dark envelopes are initial and updated envelopes, respectively.

300 overlaid on the observed data points (male - grey circle, female - red cross). The quantile levels from outer to inner envelopes are $\tau = \{.05, .1, .2, .3\}$. In particular, we look at four female infants, denoted by *A*, *B*, *C*, and *D* in Figure 5. The infant *D* is within the 90 percent quantile envelope and her brain is normally developing while the infant *C* may need further clinical investigation as she is outside the 95 percent quantile envelope. Interestingly, we find that both infants *A* and *B* are lying inside the initial 95 percent quantile envelope but are outside the updated 95 percent quantile envelope. Therefore, it may be worth to further conducting more clinical examinations to evaluate the brain development of these two infants as well.

4 Discussion

This article studies a novel estimation method in bivariate quantile varying coefficient model for functional responses based on the directional quantile concept. We approximate the varying coefficients by the B-spline basis and impose an L_2 -type penalty to achieve desired smoothness. A multistage estimation procedure is proposed based on the PS approach to borrow information from nearby directions. The PS method is capable of handling the computational complexity raised by simultaneously considering multiple directions to efficiently estimate varying coefficients while guaranteeing certain smoothness along directions. The proposed objective function is reformulated into a new form and then the ADMM is utilized to solve the optimization problem. Simulation studies demonstrate that the our proposed method is more efficient in constructing directional quantile envelopes. Moreover, it provides quantile envelopes with not only desired smoothness but also more accurate coverage rates. We analyze a real data on DTI properties and our analysis yields new insights are provided on the early brain development at both population and individual levels.

There are several topics that merit further research. The asymptotic properties, such as consistency and asymptotic normality, of our proposed method could be developed. In particular, the asymptotic properties of (11) may be studied by using the techniques in Li *et al.* (2007). In the multistage estimation procedure, similar regular conditions in Zhu *et al.* (2014) could be imposed to pursue its asymptotic properties. To estimate the varying coefficients, other basis functions, for example, wavelet basis, could be used (Tsatsanis and Giannakis, 1993; Ramsay and Silverman, 2005). Another alternative is to use local kernel polynomial smoothing method (Fan and Gijbels, 1996; Zhu *et al.*, 2012). To achieve certain properties of the varying coefficients in (11), other penalty functions can be adapted; for instance, LASSO, SCAD or MCP can be used to yield sparse estimates of the B-spline basis (Tibshirani, 1996; Fan and Li, 2001; Zhang, 2010). Furthermore, our estimation method can be easily extended to multivariate quantile varying coefficient model for functional responses (Kong and Mizera, 2012; Zhu *et al.*, 2012) by modifying the multistage estimation procedure.

References

- Abdous, B. and Theodorescu, R. (1992). Note on the spatial quantile of a random vector. *Statistics & Probability Letters*, **13**(4), 333–336.
- Boyd, S., Parikh, N., Chu, E., Peleato, B., and Eckstein, J. (2011). Distributed optimization and statistical learning via the alternating direction method of multipliers. *Foundations and Trends in Machine Learning*, **3**(1), 1–122.
- Bradic, J., Fan, J., and Wang, W. (2011). Penalized composite quasi-likelihood for ultrahigh dimensional variable selection. *Journal of the Royal Statistical Society: Series B*, **73**(3), 325–349.
- Breckling, J. and Chambers, R. (1988). M-quantiles. *Biometrika*, **75**(4), 761–771.
- Cai, Z. and Xu, X. (2008). Nonparametric quantile estimations for dynamic smooth coefficient models. *Journal of the American Statistical Association*, **103**(484).
- Chaudhuri, P. (1996). On a geometric notion of quantiles for multivariate data. *Journal of the American Statistical Association*, **91**(434), 862–872.
- Fan, J. and Gijbels, I. (1996). *Local polynomial modelling and its applications: monographs on statistics and applied probability 66*, volume 66. CRC Press.
- Fan, J. and Li, R. (2001). Variable selection via nonconcave penalized likelihood and its oracle properties. *Journal of the American statistical Association*, **96**(456), 1348–1360.
- Fan, J., Yao, Q., and Cai, Z. (2003). Adaptive varying-coefficient linear models. *Journal of the Royal Statistical Society: Series B*, **65**(1), 57–80.
- Gabay, D. and Mercier, B. (1976). A dual algorithm for the solution of nonlinear variational problems via finite element approximation. *Computers & Mathematics with Applications*, **2**(1), 17–40.
- Guo, M., Zhou, L., Huang, J. Z., and Härdle, W. K. (2015). Functional data analysis of generalized regression quantiles. *Statistics and Computing*, **25**(2), 189–202.

- Hallin, M., Paindaveine, D., Šiman, M., Wei, Y., Serfling, R., Zuo, Y., Kong, L., and Mizera, I. (2010). Multivariate quantiles and multiple-output regression quantiles: From l optimization to halfspace depth [with discussion and rejoinder]. *The Annals of Statistics*, **38**(2), 635–703.
- Hastie, T. and Tibshirani, R. (1993). Varying-coefficient models. *Journal of the Royal Statistical Society. Series B*, **55**(4), 757–796.
- Hestenes, M. R. (1969). Multiplier and gradient methods. *Journal of optimization theory and applications*, **4**(5), 303–320.
- Honda, T. (2004). Quantile regression in varying coefficient models. *Journal of Statistical Planning and Inference*, **121**(1), 113–125.
- Huang, J. Z., Wu, C. O., and Zhou, L. (2002). Varying-coefficient models and basis function approximations for the analysis of repeated measurements. *Biometrika*, **89**(1), 111–128.
- Huang, J. Z., Wu, C. O., and Zhou, L. (2004). Polynomial spline estimation and inference for varying coefficient models with longitudinal data. *Statistica Sinica*, **14**(3), 763–788.
- Kim, M.-O. (2007). Quantile regression with varying coefficients. *The Annals of Statistics*, **35**(1), 92–108.
- Koenker, R. (2005). *Quantile regression*. Cambridge University Press.
- Koenker, R. and Bassett, G. (1978). Regression quantiles. *Econometrica*, **46**(1), 33–50.
- Koenker, R. and Park, B. J. (1996). An interior point algorithm for nonlinear quantile regression. *Journal of Econometrics*, **71**(1), 265–283.
- Koltchinskii, V. (1996). M-estimation and spatial quantiles. In *Robust Statistics, Data Analysis, and Computer Intensive Methods*, pages 235–250. Springer.
- Kong, L. (2009). *On multivariate quantile regression: directional approach and application with growth charts*. Ph.D. thesis, University of Alberta.
- Kong, L. and Mizera, I. (2012). Quantile tomography: Using quantiles with multivariate data. *Statistica Sinica*, **22**, 1589–1610.

- Kong, L. and Zuo, Y. (2010). Smooth depth contours characterize the underlying distribution. *Journal of Multivariate Analysis*, **101**(9), 2222–2226.
- Li, Y., Liu, Y., and Zhu, J. (2007). Quantile regression in reproducing kernel hilbert spaces. *Journal of the American Statistical Association*, **102**(477), 255–268.
- Li, Y., Zhu, H., Shen, D., Lin, W., Gilmore, J. H., and Ibrahim, J. G. (2011). Multi-scale adaptive regression models for neuroimaging data. *Journal of the Royal Statistical Society: Series B*, **73**(4), 559–578.
- Lin, Z., Chen, M., and Ma, Y. (2013). The augmented lagrange multiplier method for exact recovery of corrupted low-rank matrices. arXiv:1009.5055.
- Polzehl, J. and Spokoiny, V. (2006). Propagation-separation approach for local likelihood estimation. *Probability Theory and Related Fields*, **135**(3), 335–362.
- Polzehl, J. and Spokoiny, V. G. (2000). Adaptive weights smoothing with applications to image restoration. *Journal of the Royal Statistical Society: Series B*, **62**(2), 335–354.
- Powell, M. J. (1967). *A method for non-linear constraints in minimization problems*. UKAEA.
- Ramsay, J. and Silverman, B. (2005). *Functional Data Analysis*. Springer, 2nd edition.
- Ronkainen, T., Oja, H., and Orponen, P. (2003). Computation of the multivariate Oja median. In *Developments in robust statistics*, pages 344–359. Springer.
- Small, C. G. (1990). A survey of multidimensional medians. *International Statistical Review/Revue Internationale de Statistique*, **58**(3), 263–277.
- Tang, Y., Wang, H. J., and Zhu, Z. (2013). Variable selection in quantile varying coefficient models with longitudinal data. *Computational Statistics & Data Analysis*, **57**(1), 435–449.
- Tibshirani, R. (1996). Regression shrinkage and selection via the lasso. *Journal of the Royal Statistical Society. Series B*, **58**(1), 267–288.

- Tsatsanis, M. K. and Giannakis, G. B. (1993). Time-varying system identification and model validation using wavelets. *Signal Processing, IEEE Transactions on*, **41**(12), 3512–3523.
- Tukey, J. W. (1975). Mathematics and the picturing of data. In *Proceedings of the international congress of mathematicians*, volume 2, pages 523–531.
- Wang, H. J., Zhu, Z., and Zhou, J. (2009). Quantile regression in partially linear varying coefficient models. *The Annals of Statistics*, **37**(6B), 3841–3866.
- Wei, Y. (2008). An approach to multivariate covariate-dependent quantile contours with application to bivariate conditional growth charts. *Journal of the American Statistical Association*, **103**(481), 397–409.
- Wu, C. O., Chiang, C.-T., and Hoover, D. R. (1998). Asymptotic confidence regions for kernel smoothing of a varying-coefficient model with longitudinal data. *Journal of the American statistical Association*, **93**(444), 1388–1402.
- Yang, Y., Wang, H. J., and He, X. (2015). Posterior inference in bayesian quantile regression with asymmetric laplace likelihood. *International Statistical Review*, page to appear.
- Yu, K. and Moyeed, R. A. (2001). Bayesian quantile regression. *Statistics & Probability Letters*, **54**(4), 437–447.
- Yuan, Y. and Yin, G. (2010). Bayesian quantile regression for longitudinal studies with nonignorable missing data. *Biometrics*, **66**(1), 105–114.
- Zhang, C.-H. (2010). Nearly unbiased variable selection under minimax concave penalty. *The Annals of Statistics*, **38**(2), 894–942.
- Zhang, J.-T. and Chen, J. (2007). Statistical inferences for functional data. *The Annals of Statistics*, **35**(3), 1052–1079.
- Zhao, W., Zhang, R., Lv, Y., and Liu, J. (2013). Variable selection of the quantile varying coefficient regression models. *Journal of the Korean Statistical Society*, **42**(3), 343–358.

- Zhao, Z. and Xiao, Z. (2014). Efficient regressions via optimally combining quantile information. *Econometric theory*, **30**(06), 1272–1314.
- Zhou, X., Kong, L., Karunamuni, R., and Zhu, H. (2015). Quantile regression with varying coefficients for functional responses. Technical report, University of Alberta.
- Zhu, H., Zhang, H., Ibrahim, J. G., and Peterson, B. S. (2007). Statistical analysis of diffusion tensors in diffusion-weighted magnetic resonance imaging data. *Journal of the American Statistical Association*, **102**(480), 1085–1102.
- Zhu, H., Styner, M., Li, Y., Kong, L., Shi, Y., Lin, W., Coe, C., and Gilmore, J. H. (2010). Multivariate varying coefficient models for DTI tract statistics. In *Medical Image Computing and Computer-Assisted Intervention–MICCAI 2010*, pages 690–697. Springer.
- Zhu, H., Kong, L., Li, R., Styner, M., Gerig, G., Lin, W., and Gilmore, J. H. (2011). FADTTS: functional analysis of diffusion tensor tract statistic. *NeuroImage*, **56**(3), 1412–1425.
- Zhu, H., Li, R., and Kong, L. (2012). Multivariate varying coefficient model for functional responses. *Annals of statistics*, **40**(5), 2634–2666.
- Zhu, H., Fan, J., and Kong, L. (2014). Spatially varying coefficient model for neuroimaging data with jump discontinuities. *Journal of the American Statistical Association*, **109**(507), 1084–1098.